Project No. 12-3438

# Novel Metal Sulfides to Achieve Effective Capture and Durable Consolidation of Radionuclides

## Fuel Cycle Research and Development

**Mercouri Kanatzidis**
Northwestern University

Kimberly Gray, Federal POC
Bob Jubin, Technical POC

NEUP Nuclear Energy University Programs
U.S. Department of Energy

***Project: 3438***

# *Novel Metal Sulfides to Achieve Effective Capture and Durable Consolidation of Radionuclides*

*Technical Work Scope Identification:*
*Separations and Waste Forms (FC-1)*

*Program Supporting: FCRD*

*Prepared for*
*U.S. Department of Energy*

*By:*

*M.G. Kanatzidis, Debajit Sarma, S.S. Kota*
*Northwestern University*
*&*

*B.J. Riley, D.A. Pierce, and J. Chun*
*Pacific Northwest National Laboratory*

*Final report January 30, 2016*

**SUMMARY**

This report documents the work done under NEUP grant to examine the capability of novel chalcogels and some binary metal chalcogenides as a host matrix for the capture of gaseous iodine and the feasibility of their iodine-laden materials to be converted into a permanent waste form.

The presented work was conducted over last two years. A number of novel chalcogels $Zn_2Sn_2S_6$, $Sb_4Sn_4S_{12}$, $NiMoS_4$, $CoMoS_4$, antimony sulfide ($SbS_x$) chalcogels, silver functionalized chalcogels and binary metal sulfides ($Sb_2S_3$) were developed and studies for their iodine absorption efficacies. A new and simple route was devised for the large scale preparation of antimony sulfide chalcogel. The chalcogel was obtained by treating $Sb_2S_3$ with $Na_2S$ in the presence of water followed by addition of formamide. The obtained gels have a low-density sponge like network of meso porous nature having BET surface area of 125 $m^2/g$.

The chalcogels, silver functionalized chalcogel and the binary metal sulfides were exposed to iodine vapors in a closed container. Silver-functionalized chalcogels and $Sb_2S_3$ powders showed iodine uptake up to 100 wt%, the highest iodine uptake of 200 wt% was observed for the SbS-III chalcogel. The PXRD patterns of iodine-laden specimens revealed that iodine shows spontaneous chemisorption to the matrix used.

The iodine loaded chalcogels and the binary chalcogenides were sealed under vacuum in fused silica ampoules and heated in a temperature controlled furnace. The consolidated products were analyzed by PXRD, energy dispersive spectroscopy (EDS), UV-Vis and Raman spectroscopy. The final products were found to be amorphous in most of the cases with high amount (~4-35 wt%) of iodine and aapproximately ~60- 90 % of the absorbed iodine could be consolidated into the final waste form.

Alginate reinforced composite scaffolds with SbS/SnS chalcogels and $Sb_2S_3$ bulk powder were also fabricated aiming to study their efficacy as host matrices in capturing the gaseous molecular iodine in dynamic mode from nuclear spent fuel. The obtained composites looks robust in comparison to their respective pristine chalcogels and $Sb_2S_3$ bulk powder.

## CONTENTS

## ABBREVIATIONS, SYMBOLS AND NOMECLATURE

BET Brunauer-Emmett-Teller

BJH Barrett-Joyner-Halenda

CoMoS $CoMoS_4$

CoMoS-Ag Silver functionalized $CoMoS_4$

CoSbS $Co_3Sb_2S_6$

DTA Differantial thermal analysis

EDS Energy dispersive spectroscopy

FM Formamide

FY Fiscal year

HSAB Hard soft acid base

IR Infrared

$I_2(g)$ Iodine gas

NiMoS $NiMoS_4$

NiMoS-Ag Silver functionalized $NiMoS_4$

NiSbS $Ni_3Sb_2S_6$

PVP Polyvinylpyrrolidone

PXRD X-ray diffraction

$Sb_2S_3I$ Iodine loaded $Sb_2S_3$

SbS-I $Sb_3[SbS_3]_3$

SbS-II $SbS_x$

SbS-III $SbS_x$

SbS-IV $SbS_x$

SbS-V $SbS_x$

SbSnS $Sb_4Sn_3S_{12}$

SbSnS-Ag Silver functionalized $Sb_4Sn_3S_{12}$

SEM Scanning electron microscopy

STEM Scanning transmission electron microscopy

TGA Thermogravimetric analysis

TEM Transmission electron microscopy

$t_{1/2}$ half-life time

UV-vis Ultraviolet-visible

ZnSnS $Zn_2Sn_2S_6$

ZnSnS-Ag Silver functionalized $Zn_2Sn_2S_6$

ZnSnS $Zn_2Sn_2S_6$ Chalcogel

## 1 INTRODUCTION

World energy consumption is rising due to ever increasing population and improved standards of living. Especially, demand for electricity is rising at a very fast rate, twice as fast as overall energy demand. Nuclear power produces electricity in a most environmentally benign way without emitting any pollutants. Nuclear energy accounts for 11% of the world's electricity and almost 20% of the electricity in USA.[1-2] Though nuclear energy is efficient and clean, the waste products generated during the nuclear power production should be safely disposed.[3]

In nuclear power plants, during the nuclear fission process, volatile radionuclides such as tritium ($^{3}$H), technetium ($^{99}$Tc), krypton ($^{85}$Kr), iodine-129 ($^{129}$I), and iodine-131 ($^{131}$I) are generated.[4] Among these radionuclides, $^{129}$I poses a major long-term risk due to its long half-life ($t_{1/2}$ = 1.6×10$^{7}$ years) and its adverse health effects in humans. Currently, in nuclear energy community, there is a strong interest to find a suitable matrices to capture radio iodine. To capture the radio iodine, different host matrices were appraised and the resultant iodine laden host matrices were assayed to consolidate into a permanent waste. The most common matrices studied were the silver composites such as silver incorporated zeolites and mordenites.[5] On exposure to iodine, silver from the zeolite and mordenite matrices, converts iodine to stable AgI form. Prior to the deposition in geological repository, such AgI-embedded host matrices should be converted in to a permanent waste form.

Based on hard soft acids base (HSAB) principle, chalcogenide and chalcogenide-based aerogels (*chalcogels*),[6-9] are expected to be a good sorbent material for $I_2$, considering that $I_2$(g) is a softer Lewis acid.[10-11] Riley et al., have studied the efficacy of various chalcogels as sorbents for iodine and consolidation of the iodine loaded material into a final waste form.[11-14]

Herein we present our work on development of novel chalcogel and binary chalcogenides as iodine absorption materials and consolidation of the iodine loaded materials in order to produce a permanent waste form.

## 2 EXPERIMENTAL METHODS

### *2.1 Starting materials*

The stibnite ($Sb_2S_3$) powder, Potassium antimony tartrate ($K_2Sb_2(C_4H_2O_6)_2.3H_2O$), nickel chloride ($NiCl_2.6H_2O$), calcium chloride, cobalt chloride ($CoCl_2.6H_2O$), potassium hydroxide (KOH), Sodium sulfide nonahydrate ($Na_2S.9H_2O$), and iodine ($I_2$) were purchased from Sigma-Aldrich and used as received.

$Na_2S$ was prepared by liquid ammonia method by reacting 6.9 g (0.3 mol) of sodium with stoichiometric amount of sulfur 4.8 g (0.15 mol). $Na_3SbS_3$ was synthesized by direct combination of stoichiometric $Na_2S$, Sb and S at 700ºC in a carbon coated 9 mm diameter sealed fused silica tube. $Na_4Sn_2S_6 \cdot 14H_2O$ was prepared by reacting $SnCl_4.5H_2O$ with $Na_2S.9H_2O$ by the reported procedure.[15]

### *2.2 Preparation of chalcogels*

The chalcogels $Zn_2Sn_2S_6$ (ZnSnS), $Sb_4Sn_3S_{12}$ (SbSnS), $NiMoS_4$ (NiMoS) and $CoMoS_4$ (CoMoS) were prepared by employing metathesis reactions.[16] To prepare ZnSnS and SbSnS, Zinc acetylacetonate ($Zn(acac)_2 \cdot H_2O$) and potassium antimony tartrate ($K_2(SbC_4H_2O_6)_2 \cdot 3H_2O$) were used as metal salts and $SnS_4^{4-}$ and $Sn_2S_6^{4-}$ were used as chalcogenide clusters respectively. NiMoS and CoMoS were obtained by mixing ammonium tetrathiomolybdate [$(NH_4)_2MoS_4$] with $NiCl_2 \cdot 6H_2O$ and $CoCl_2 \cdot 6H_2O$ respectively.

We prepared the antimony sulfide chalcogels by both metathesis and hydrolysis routes.[15] The chalcogels (Figure 1) were named differently based on their synthesis condition, a brief description of the synthesis is summarized in the following equations. The detailed synthesis procedure can be found in our previous reports.[15]

$$K_2Sb_2(C_4H_2O_6)_2.3H_2O + Na_3SbS_3 + FM \rightarrow SbS\text{-}I \qquad (1)$$

$$Na_3SbS_3 + FM + H_2O \rightarrow SbS\text{-}II \qquad (2)$$

$$Sb_2S_3 + KOH + FM + H_2O \rightarrow SbS\text{-}III \qquad (3)$$

$$Sb_2S_3 + Na_2S.9H_2O + H_2O + FM \rightarrow SbS\text{-}IV \qquad (4)$$

$$K_2Sb_2(C_4H_2O_6)_2.3H_2O + Na_2S.9H_2O + H_2O + FM \rightarrow SbS\text{-}V \qquad (5)$$

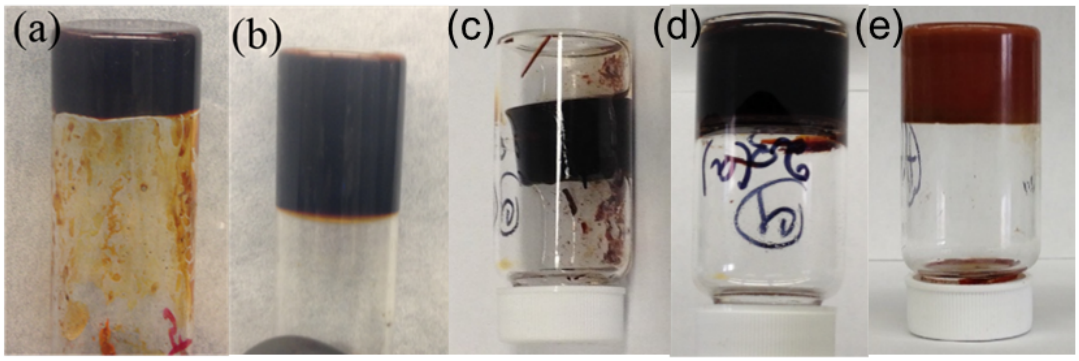


Figure 1. Photographs of the antimony sulfide wet gels (a) SbS-I, (b) SbS-II, (c) SbS-III, (d) SbS-IV, and (e) SbS-V.

In order to remove by-products, FM solvent and any unreacted precursors, the gels were washed in an ethanol and water mixture (1:1 V/V) followed by absolute ethanol for 4 days each. During the washing, soaked solvents were exchanged by fresh solvents every twelve hours. To prepare the high surface area porous gels, the solvent molecules in the gel framework were carefully replaced with air without destructing the gel structure by drying super critically at a temperature of 42°C and a pressure of 1400 psi using a Tousimis Autosamdri-815B supercritical fluid dryer. In this process, the wet monolithic gel was placed in the supercritical drying chamber and the remnant alcohol in the gel was exchanged by liquid carbon dioxide ($CO_2$) over a period of 6 hours. Fresh $CO_2$ was introduced into the chamber in every 20 minutes over the soaking period. At the end, gaseous $CO_2$ was bled very slowly to yield light mass aerogels. To obtain xerogels, after washing with ethanol, the wet gels were dried under vacuum at 50 °C. The drying of wet gels under vacuum significantly reduced their volume. The obtained dried gels were characterized by various techniques such as powder X-ray di□raction (PXRD), scanning electron microscopy (SEM), and nitrogen adsorption-desorption isotherm measurements.

### *2.3 Large scale preparation of SbS-III chalcogel*

In an attempt to prepare the SbS-III chalcogel in large quantities, $Sb_2S_3$ bulk powder was reacted with KOH in the presence of water followed by addition of formamide (FM).[17] In a typical procedure, KOH was added to $Sb_2S_3$ and mechanically mixed. The mixture was then subjected to stirring for 10-35 minutes. The resultant product was added with formamide and kept in standing without disturbing. Different reaction conditions were assayed and it resulted in the formation of gels in 2hrs.

### *2.4 SnS chalcogel*

SnS chalcogel was obtained by employing metathesis between tin chloride ($SnCl_4.2H_2O$) and sodium thiostannate ($Na_4Sn_2S_6 \cdot 14H_2O$). To form the gel, 7.5 mmol of $Na_4Sn_2S_6 \cdot 14H_2O$ was dissolved in 25 mL of water with stirring. To this solution, a separate solution of 15 mmol of $SnCl_2.2H_2O$ dissolved in 15 mL of water was slowly added. The resultant product was kept in standing without disturbing for 10 days to yield the gel.[18]

### *2.5 Preparation of silver nanoparticles*

To prepare silver nanoparticles, silver nitrate as a silver source and polyvinylpyrrolidone (PVP) as a capping agent were employed. In this process, 1 g of PVP was added to 100 mL of 20 mM $AgNO_3$ solution and stirred till the clear solution was obtained.[16] To this solution, 60 mg of NaOH and 80 mg of $Na_2CO_3$ were added and stirred till the mixture turns brown. Then, 1 g of sucrose was added and the solution was maintained at 60 °C for 2hr. At the end of the reaction, copious amounts of acetone were added to precipitate the nanoparticles. The PVP capped nanoparticles were thoroughly washed with acetone and vacuum dried.

### *2.6 Preparation of silver-functionalized chalcogels*

An amount of 35 mg of PVP-capped Ag nanoparticle powders were added to 0.2 mmol of wet ZnSnS and SbSnS gels dispersed in 20 ml of ethanol and stirred for one hour.[16] The resulting mixtures were filtered and vacuum dried. In a similar process 20 mg of PVP capped Ag nanoparticles were added to 0. 2 mmol of NiMoS (CoMoS) wet gel dispersed in 20 ml of ethanol and vacuum dried to obtain the composites.

### *2.7 Alginate-chalcogenide composites*

We prepared the alginate composites of $Sb_2S_3$ bulk powder and SbS-III and SnS chalcogels.[18] In a typical procedure, required amount of sodium alginate was dissolved in 500 ml of hot water. To alginate solution, 10 g of $Sb_2S_3$/SbS-V/SnS was added and the mixture was stirred for 15 minutes. Then the alginate-chalcogenide mixture was added with 10 g of $CaCl_2$ dissolved in 500 ml of water and stirred for 2 minutes to form the composite. The resultant composite in the solution was filtered.

### *2.8 Iodine adsorption experiment*

The iodine adsorption experiments were performed with 1g of iodine in a vial with ~ 200 mg of chalcogel/chalcogenide in a conical-shaped filter paper attached at the top of the vial in such a way that the cone was hanging towards the bottom of the vial. The vial was then kept inside a bigger vial and placed in a sand bath and maintained at 70°C. Figure 2 depicts the schematic of experimental set-up. After adsorption, iodine laden samples were taken from filter paper and weighted.

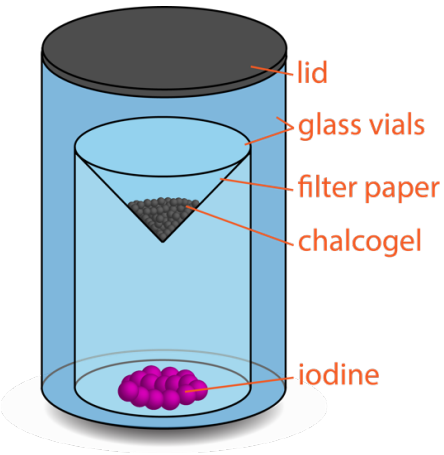


Figure 2. Schematic of iodine up-take experimental set-up.

### *2.9 Powder X-ray diffraction*

The powder X-ray diffraction (PXRD) patterns were collected with a CPS 120 INEL X-ray powder diffractometer with a graphite monochromated Cu Kα radiation operating at 40 kV and 20 mA. The samples were prepared by grinding and spreading over a glass slide.

### *2.10 Scanning electron microscopy and energy dispersive spectroscopy*

The energy dispersive spectroscopy (EDS) was performed with a Hitachi S-3400N-II scanning electron microscope (SEM) equipped with an ESED II detector. An accelerating voltage of 20 kV and 60 seconds acquisition time was applied for elemental analysis.

### *2.11 Nitrogen adsorption-desorption isotherm measurements*

These measurements were carried out to measure the surface areas of chalcogels using Micromeritics Tristar II system at 77 K. Prior to the analysis, the chalcogel was degassed at 350 K under vacuum for 20 hours to remove any adsorbed impurities. Surface area and distribution

of pore sizes were estimated from Brunauer-Emmett-Teller (BET) and Barrett-Joyner-Halenda (BJH) models, respectively.

### *2.12 Raman spectroscopy*

A DeltaNu Raman system that uses a 785 nm CW laser was used to record the Raman spectra of the grounded samples. The spectra was collected in the spectral range of 100 – 2000 $cm^{-1}$ using a 0.5 mm capillary tube.

### *2.13 Band gap measurements*

The UV-vis/near-IR diffuse reflectance spectra were collected using a Shimadzu UV03010 PC double beam, double monochromator spectrophotometer in the wavelength range of 200-2500 nm. $BaSO_4$ powder was used as a reference and base material on which the grinded powder sample was coated. The reflectance data was converted to absorption data using Kubelka-Munck equation. The band edge of the sample was calculated from the intercept of the line extrapolated from the high energy end to the baseline.

### *2.14 Thermogravimetric analysis*

The thermogravimetric analysis (TGA) was performed with a Shimadzu TGA-50 system under nitrogen atmosphere in an aluminum crucible. The analysis was performed with a heating rate of 10 °C/min and a nitrogen flow rate of 40 mL/min from room temperature to 600 °C.

### *2.15 Differential thermal analysis*

The differential thermal analysis (DTA) were performed on a Shimadzu DTA-50 thermal analyzer. For a typical analysis, around 30 mg of sample was sealed in a quartz ampoule and sealed under vacuum, another sealed quartz ampoule with $Al_2O_3$ was used as reference material. The analysis was performed with a heating rate of 2 °C/min and a nitrogen flow rate of 30 mL/min from room temperature to required temperature.

### *2.16 Consolidation experiments*

The consolidation experiments of the iodine-adsorbed chalcogels were carried out in evacuated and sealed fused silica ampoules (9 mm diameter). The iodine loaded materials in the ampules were then heated in a temperature controlled furnace from room temperature to required temperature.

## 3 RESULTS AND DISCUSSION

### *3.1 Silver functionalized chalcogels*

The characterization of silver functionalized chalcogels and their iodine laden materials were discussed in detail in previous report.[16] The PXRD patterns of iodine laden silver functionalized chalcogel shows the presence of AgI where ZnSnS-Ag and SbSnS-Ag also showed the presence $SnI_4$ and $SbI_3$ respectively. The TGA data of iodine laden ZnSnS-Ag and SbSnS-Ag showed weight loss up to 50 % and NiMoS-Ag and CoMoS-Ag showed 10-20 % weight loss. The weight loss in iodine laden ZnSnS-Ag and SbSnS-Ag can be attributed to volatilization of $SnI_4$ and $SbI_3$ which have been shown to form due to chemisorption of iodine on respective chalcogels. The weight loss in iodine laden NiMoS-Ag and CoMoS-Ag is due to loss of physisorbed iodine and the decomposition of NiMoS and CoMoS.[16]

### *3.2 NiSbS and CoSbS chalcogels*

The NiSbS and CoSbS are powders and black in color. The SEM micrographs shows that both are non-porous and EDS reveals that NiSbS (CoSbS) mainly contains nickel (cobalt), antimony and sulfur along with the presence of sodium ~ 3-6 at%. From EDS, the average composition of NiSbS and CoSbS can be written as $NaNi_6Sb_{2.5}S_{10}$ and $NaCo_{6.6}Sb_{5.7}S_{15.4}$ respectively.[15] This indicates that the Ni (Co) ions do not fully neutralize the antimony sulfide anion ($SbS_3^{3-}$) and the Ni (Co)/$SbS_3$ network has a residual anionic charge which is balanced by sodium ions. PXRD patterns of the NiSbS and CoSbS showed the broad features along with a few crystalline peaks in NiSbS and the presence of weak peaks in CoSbS.

### *3.3 Antimony sulfide*

The $Sb_2S_3$ powder show high iodine uptake capacity and the iodine loaded powder appears to be dark red-brown in color.[19] The powder X-ray diffraction (PXRD) of the iodine loaded stibnite powder ($Sb_2S_3I$) shows that the primary phase is $SbI_3$ and few other small peaks can be assigned to the $SbI_3(S_8)_3$. The TGA of the iodine loaded stibnite powder ($Sb_2S_3I$) shows ~ 47 % weight loss at 200 ºC and another ~ 13 % weight loss at 350 ºC. The SEM and EDS analysis of the iodine loaded stibnite powder ($Sb_2S_3I$) shows the presence of Sb, S and I. The

highest content of iodine was found to be 67 wt % by EDS but in most of the cases it was ~50 wt %.

### *3.4 Antimony sulfide chalcogels*

The aero and xero gels of SbS-I and SbS-II look red in color and the aerogels are fluffy in nature. The SEM micrographs indicate that aerogels are spongy in nature and porous whereas the xerogels are non-porous. EDS data of SbS-I showed the presence of antimony, sulfur, sodium and potassium while EDS of SbS-II showed antimony, sulfur and sodium.[15] However antimony and potassium lines overlap in EDS of SbSb-I. From EDS the average elemental compositions of SbS-I and SbS-II can be written as $KNa_3Sb_{30}S_{36}$ and $NaSb_{7.5}S_{11}$ respectively. In both the samples sodium is the part of material which neutralizes the residual anionic charge in the network. Potassium in SbS-I, can be either part of the material like sodium which neutralizes the residual anionic charge or appeared from the overlap of antimony L, and potassium K lines in EDS. The PXRD patterns of both the aero and xero gels of SbS-I and SbS-II mainly showed the presence of broad peaks along with a few sharp peaks which could not be matched with any known crystalline phases. The presence of dominant broad features clearly indicate the lack of long range order which is typical characteristic of the chalcogels.

The porosities of the chalcogels were evaluated by $N_2$ adsorption at 77 K and surface area values were calculated with the BET model. BET analysis inferred that the aerogels of SbS-I and SbS-II are mesoporous in nature with specific surface areas in the range of 250 $m^2/g$. The BJH average pore diameter of the SbS-I and SbS-II are in the range of 10-12 nm and 16-19 nm respectively. Figure 3 represents the typical nitrogen adsorption and desorption isotherms of the SbS-I and SbS-II aerogels. UV-Vis diffuse reflectance spectroscopy of SbS-I and SbS-II show the same band gap energies at 1.5 eV indicating that these materials absorb light in the near infra-red region.

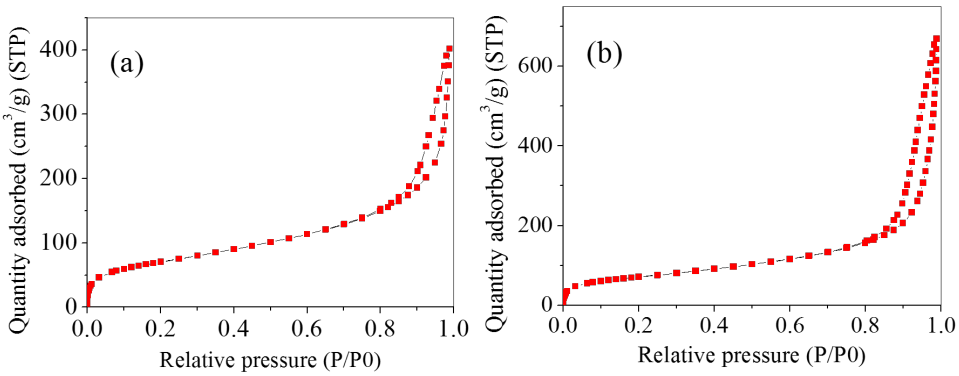


Figure 3. Nitrogen adsorption and desorption isotherms of (a) SbS-I and (b) SbS-II aerogels.

The TGA studies of both the chalcogels were most stable with weight losses of only ~10 % after heating to 600 °C and comply the same trend. The weight loss at early stage up to 200 °C corresponds to loss of residual solvent left from the synthesis of gel and the weight loss above 500 °C can be attributed to the thermal decomposition of the chalcogel network.

### *3.5 Iodine adsorption experiments*

To evaluate the efficacy of SbS-I and SbS-II chalcogels as a host matrix for the capture of radioactive iodine, we have carried out the iodine adsorption study on SbS-I and SbS-II xerogels at 60 ºC. The iodine uptake values are 75 wt% and 100 wt % for SbS-I and SbS-II respectively. EDS analysis of both the iodine laden SbS-I and SbS-II showed the presence of Sb, S and iodine. SEM micrographs collected from all the locations showed the presence of hexagonal plates which was found to be $SbI_3$ from EDS analysis. The PXRD pattern of iodine laden samples could be matched with $SbI_3$. TGA traces of both the iodine laden SbS-I and SbS-II show the weight losses at same temperatures around 220 ºC and at 330 ºC. The iodine uptake values of the SbS-I and SbS-II chalcogels are consistent with the uptake values of $Sb_2S_3$ powders and the PXRD and TGA results of iodine laden SbS-I and SbS-II are very similar with those of $Sb_2S_3$-iodine laden samples.

### *3.6 Antimony sulfide chalcogel (SbS-III)*

The xero gel of SbS-III looks red in color and fluffy in nature.[20] To know the morphology and composition of the sample, SEM and EDS analyses were carried out. Figure 4 shows the SEM micrographs and the corresponding EDS data of SbS-III xerogel. EDS data showed the presence of antimony, sulfur and potassium, however antimony and potassium lines overlap.

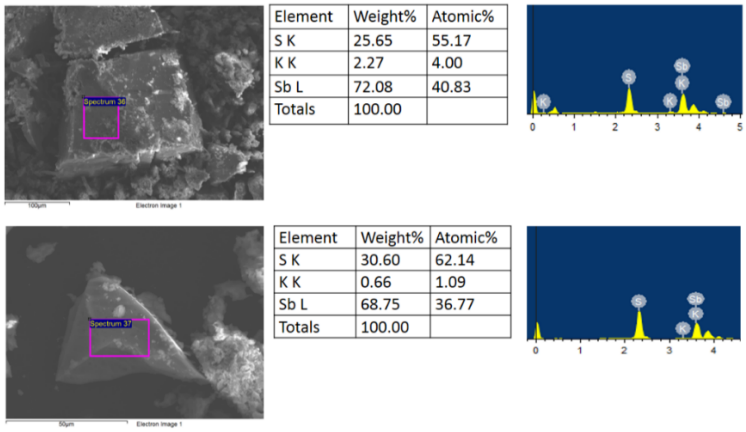

| Element | Weight% | Atomic% |
|---|---|---|
| S K | 25.65 | 55.17 |
| K K | 2.27 | 4.00 |
| Sb L | 72.08 | 40.83 |
| Totals | 100.00 | |

| Element | Weight% | Atomic% |
|---|---|---|
| S K | 30.60 | 62.14 |
| K K | 0.66 | 1.09 |
| Sb L | 68.75 | 36.77 |
| Totals | 100.00 | |

Figure 4. SEM micrographs and the corresponding EDS data of SbS-III xerogel.

The PXRD pattern (Figure 5a) mainly showed the presence of broad peaks along with a few sharp peaks which could not be matched with any known crystalline phases. The presence of dominant broad features clearly indicate the lack of long range order which is typical characteristic of the chalcogels. BET analysis inferred that the xerogels of SbS-III are mesoporous in nature with specific surface areas in the range of 12 $m^2/g$.

The weight difference from before and after iodine adsorption showed the iodine uptake value is ~ 200 wt%. This uptake value is close to that of ZnSnS, SbSnS and much better that bulk $Sb_2S_3$ powder. The EDS analysis of the iodine laden SbS-III showed the presence of Sb, S and iodine and the iodine uptake from EDS analysis in agreement with the uptake values obtained from weight difference. Figure 5b shows the PXRD patterns of iodine laden SbS-III, the pattern could be matched with $SbI_3$.

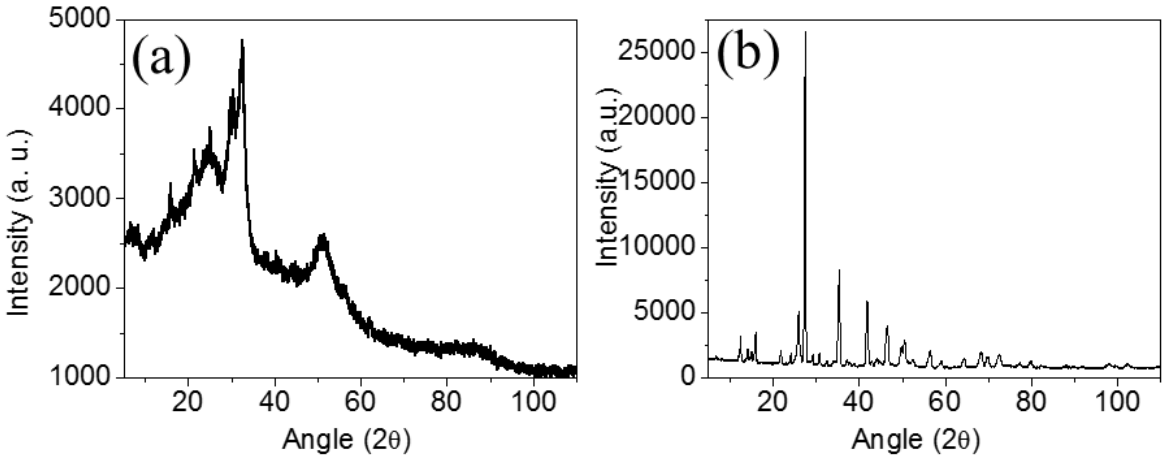


Figure 5. PXRD pattern of (a) SbS-III xerogel and (b) iodine loaded SbS-III.

Encouraged with the efficacy of SbS-III chalcogel (~ 200 wt % uptake) as a host matrix to capture the iodine, we thought it would be worthwhile to optimize its synthetic procedure to produce in large quantities. For this purpose, $Sb_2S_3$ bulk powder was treated with KOH under different experimental conditions.[17] The best results were obtained for the 50 : 50 wt% of $Sb_2S_3$:KOH in 1:1 H2O: FM synthesis condition (SbS-e). The SEM micrographs of SbS-e chalcogel reveal that it consists of forests of micro rods and high resolution imaging infers that the length and diameter of the rods are around 3 µm and 300 nm respectively (Figure 6). EDS analyses show that the composition is similar to that of SbS-III xerogel containing mainly Sb and S along with the presence of 1-3 at % of potassium. From EDS, the average elemental compositions of SbS-e can be written as $K_{2.5}Sb_{14.5}S_{24}$.

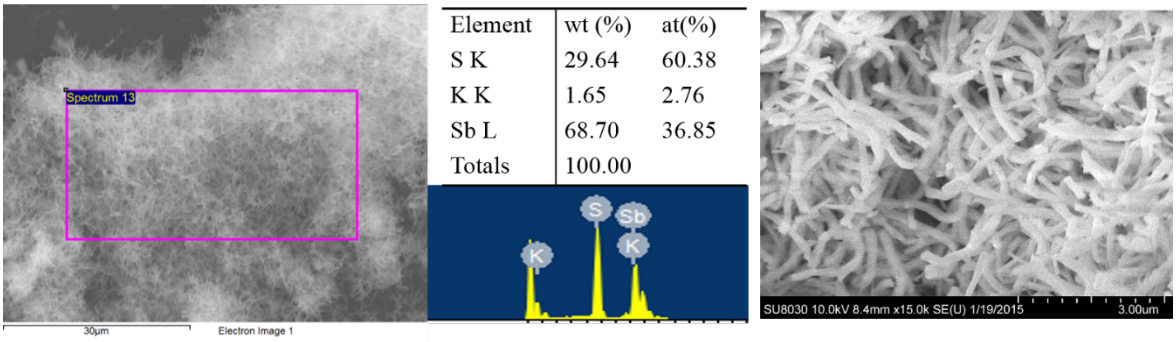


Figure 6. SEM micrographs and EDS data of the SbS-e chalcogel.

### *3.7 SbS-IV chalcogel*

The aero and xero gels of SbS-IV look red in color while aerogel is fluffy in nature. The SEM micrographs indicate that aerogels are spongy in nature whereas the xerogel looks dense. EDS data of SbS-IV showed mainly the presence of antimony and sulfur along with 2-4 at % of sodium. From EDS, the average elemental composition of SbS-IV can be written as $NaSb_{12.7}S_{19.7}$. Sodium is the part of material which neutralizes the residual anionic charge in the chalcogel network. The PXRD pattern mainly showed the presence of broad peaks. The presence of dominant broad features clearly indicate the lack of long range order which is typical characteristic of the chalcogels. The BET analysis inferred that SbS-IV aerogel exhibits high specific surface area of 125 $m^2/g$ with mesoporous in nature whereas xerogels show specific surface area of 30 $m^2/g$.

### *3.8 SbS-V chalcogel*

The aero and xero gels of SbS-V look red in color while the aerogel is fluffy in nature. Most of the regions of both the xero and aerogels of SbS-V comprise network of micro fibers and the rest contain micro rods having length from 100 μm to 200 μm.[18] STEM micrographs (Figure 7) also indicate that SbS is composed of bundles of micro fibers. EDS analyses show that the composition of micro fibers is similar to that of other SbS chalcogels (SbS-I, SbS-II and SbS-III) containing mainly Sb and S along with the presence of residual potassium and sodium. Micro rods exhibit the irregular compositions and not consistent with the sample location from where the EDS data collected.

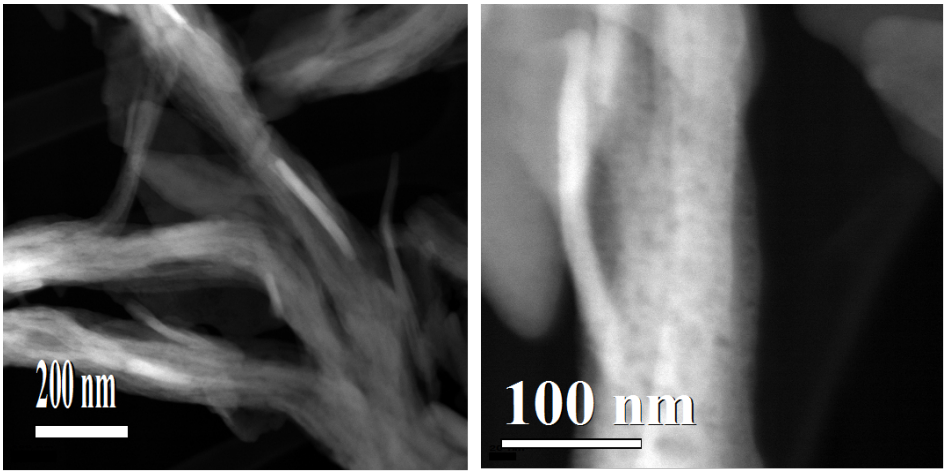


Figure 7. STEM micrographs of SbS-V aerogel.

The microstructure of the chalcogel was analyzed by TEM imaging and representative micrographs are shown in Figure 8a-c. High resolution TEM micrographs infer that the observed SbS micro fibers consists of bundles of nanowires, nanotubes and nano onions.

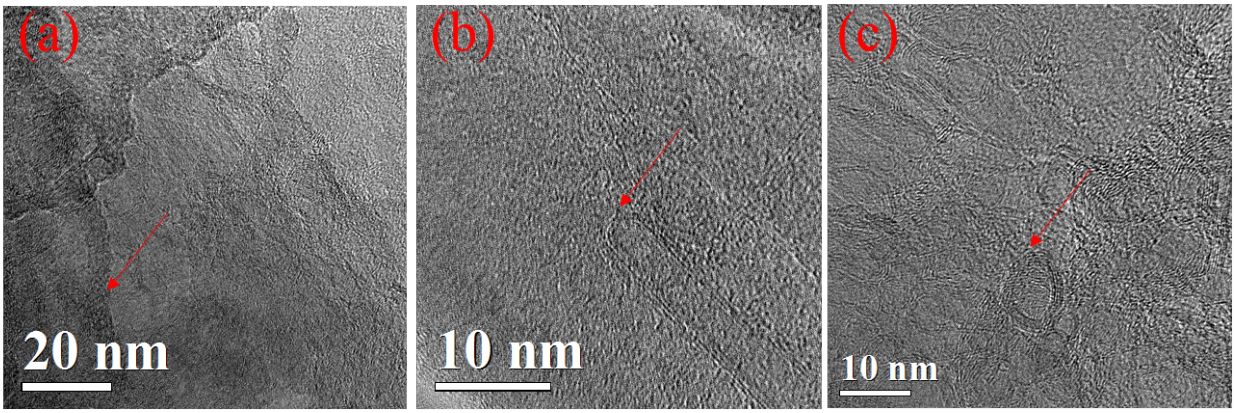


Figure 8. TEM micrographs of SbS-V aerogel. The bundles of nanowires, nanotubes and nano onions are shown in (a), (b) and (c) respectively by red arrowheads.

The PXRD pattern mainly showed the presence of broad peaks with a few sharp peaks, which might be emerged from the micro rods present in the sample. UV-Vis diffuse reflectance spectroscopy of SbS-V show the band gap of 1.75 eV matching with those of other SbS chalcogels and indicating that these materials absorb light in the near infra-red region. BET analysis revealed that both the aero and xero gels of SbS-V exhibit surface areas in the range of 10-20 $m^2/g$

### *3.9 Composites of $Sb_2S_3$, SbS and SnS with alginate*

We prepared the alginate reinforced composite matrices with $Sb_2S_3$ bulk powder and SbS-III and SnS xerogels.[18] $Sb_2S_3$ was purchased from sigma Aldrich while the reaction of $Sb_2S_3$ with KOH and addition of FM resulted the formation of SbS-III chalcogel. SnS chalcogel was synthesized by employing metathesis technique and characterized utilizing different techniques. From SEM micrographs, the SnS xerogel looks non spongy and EDS data collected from multiple sample locations mainly showed the presence of Sn and S along with residual sodium. From EDS data, the composition of SnS can be written as $Na_{0.03}Sn_2S_{3.2}$. The powder XRD pattern of the SnS xerogel predominantly shows the presence of broad diffuse features. BET analysis inferred that SnS xerogel is mesoporous in nature with specific surface area of 13 $m^2/g$. The observed BET surface area is correspond to the silica equivalent surface areas of 144 $m^2/g$.

In order to utilize as a host matrice to capture the iodine in a dynamic mode from nuclear spent fuel, composites of $Sb_2S_3$, SbS-V and SnS chalcogels were fabricated using alginate as a filler. For this purpose, 2 wt % of alginate was dispersed in SbS-V and SnS chalcogels while $Sb_2S_3$ was reinforced with 2-5 w % of alginate. The obtained composites look robust in comparison to their respective native counterparts and their photographs are shown in Figure 9.

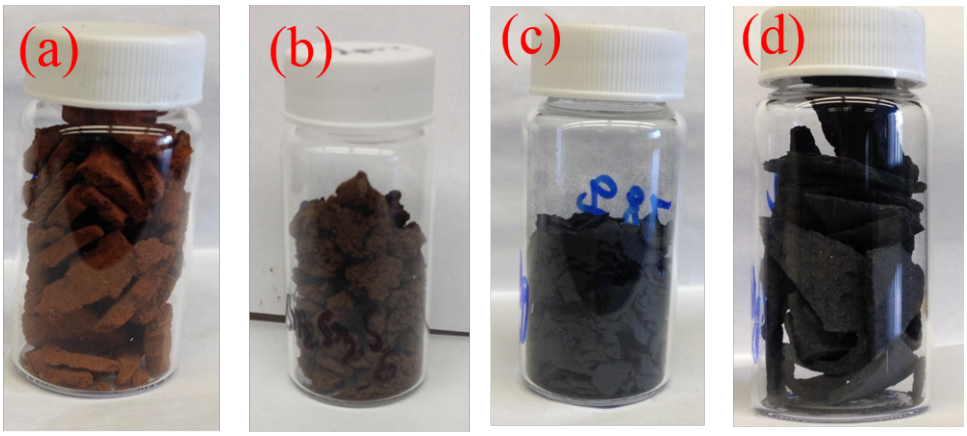


Figure 9. The photographs of (a) SbS-III and (b) SnS chalcogel composites with 2 wt % of alginate and $Sb_2S_3$ composites with (c) 2 wt % and (d) 5 wt % of alginate.

### *3.10 Consolidation*

The iodine laden samples were loaded inside a 9 mm diameter fused silica tube and then sealed under vacuum. During this process, in order to prevent any loss of adsorbed iodine the tube was kept immersed into liquid $N_2$. The iodine loaded materials in the ampules were then heated in a temperature controlled furnace from room temperature to required temperature.

#### *3.10.1 Iodine loaded silver functionalized chalcogels*

The consolidation of iodine laden silver functionalized chalcogels shows no indication of glass formation.[16] The AgI was separated from the chalcogel matrix yielding to the formation of black residue at the bottom and along with the decomposed chalcogel matrix.

It was evident that the heat treatment of the iodine laden chalcogels without any glass forming additives resulted in separation of the iodine from the matrix and subsequent decomposition of the chalcogel matrix. Hence to overcome this problem binary sulfide ($Sb_2S_3$/$As_2S_3$) additives were used for the consolidation of the iodine loaded chalcogels.

#### *3.10.2 Iodine loaded $Sb_2S_3$ consolidation*

The consolidation of iodine loaded $Sb_2S_3$ ($Sb_2S_3I$) was performed in a temperature controlled furnace. For this purpose four consolidation experiments were performed with (a) 1:1 (100 mg $Sb_2S_3I$ + 50 mg $Sb_2S_3$), (b) 1:3 (100 mg $Sb_2S_3I$ + 150 mg $Sb_2S_3$), (c) 1:4 (100 mg $Sb_2S_3I$ + 200 mg $Sb_2S_3$), and (d) 1:5 (100 mg $Sb_2S_3I$ + 250 mg $Sb_2S_3$) molar ratios of Sb in $Sb_2S_3I$ and $Sb_2S_3$.[19] The experiments were done using the same procedure as above in a fused silica ampoule at 600°C followed by water quenching.

The PXRD of the consolidated product in all the cases shows the formation of an amorphous phase. The SEM and EDS data shows the presence of Sb, S and I in the consolidated product. Around 11 – 21 wt % of iodine could be found in the consolidated product by EDS.

The consolidation of the iodine loaded stibnite ($Sb_2S_3I$) with added $Sb_2S_3$ showed the formation of an amorphous phase after the heat treatment at 600°C. The glass phase after the consolidation was characterized using TGA, DTA, band gap measurement and Raman spectroscopy.

The band gap of the consolidated product was found to be 1.8 eV from the Uv-Vis/Near-IR spectrum (Figure 10a). The Raman spectra of the consolidated product shows four distinct peaks at 106, 140, 251 and 315 $cm^{-1}$ (Figure 10b). The band gap and peaks in the Raman spectra are in good agreement with the values reported in the literature for the SbSI glass phases.[21-22] The thermogravimetric analysis (TGA) of the consolidated product shows that it is stable up to 300°C, after which it loses 25 wt % in the temperature range of 300-350°C (Figure 10c). This weight loss can be attributed to escape of iodine as $SbI_3$ from the glass form. The differential thermal analysis (DTA) shows that the glass melts at ~385°C on heating and crystalizes at ~365°C while cooling (Figure 10d).

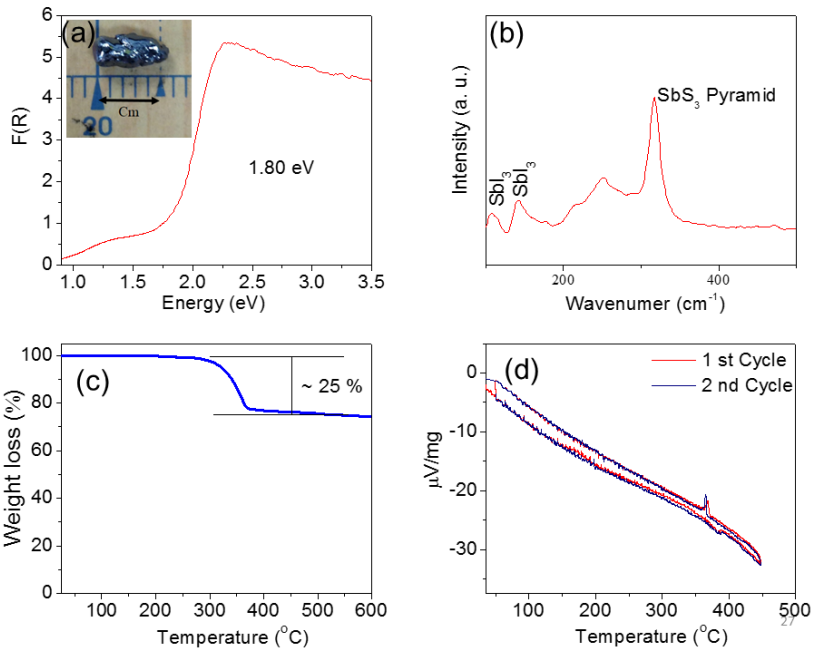


Figure 10. (a) UV-Vis/near-IR spectrum, the inset shows the consolidated product, (b) Raman spectrum, (c) the TGA and (b) the DTA data of the consolidated product.

*3.10.3 Iodine laden chalcogel (SbS-III) consolidation*

The iodine absorption capacity of the $Sb_2S_3$ powders were increased by two folds in the chalcogel forms (SbS-III). The consolidation of iodine laden chalcogel (SbS-III) were performed with added binary sulfides ($Sb_2S_3$/$As_2S_3$) on top of the iodine laden materials without mixing. The fused silica ampoules were than evacuated, sealed and heated from room temperature to required temperature followed by water quenching.

*3.10.3.1 Iodine laden chalcogel (SbS-III) consolidation with $Sb_2S_3$*

The consolidation of the iodine laden chalcogel (SbS-III) was explored with different weight percentage of $Sb_2S_3$ powder.[20] For this purpose four consolidation experiments were performed with (a) 50:50, (b) 40:60, (c) 33:67 and (d) 25:75 weight percentage of iodine laden chalcogel and $Sb_2S_3$ respectively. The experiments were done using the same procedure as above in a fused silica ampoule at 600°C followed by water quenching (Figure 11).

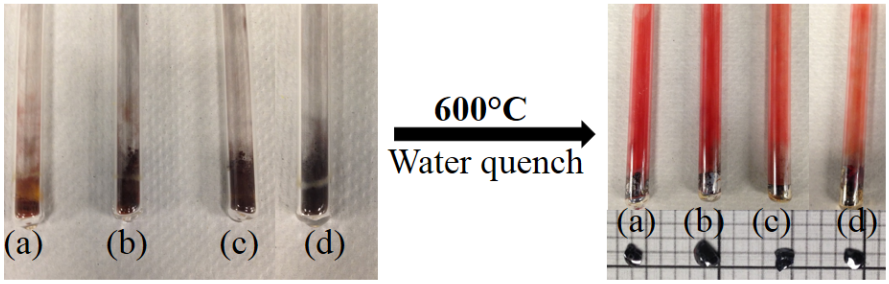


Figure 11. Picture of iodine loaded chalcogel and $Sb_2S_3$ in varying weight percentage, before (left) and after (right) heat treatment at 600°C. Bottom right shows the pieces of the consolidated product obtained from the respective experiments.

The PXRD of the consolidated product in all the four cases shows the formation of an amorphous phase (Figure 12). The SEM and EDS data shows the presence of Sb, S and iodine in the consolidated product. Around 16 – 27 wt % of iodine could be found in the consolidated products by EDS.

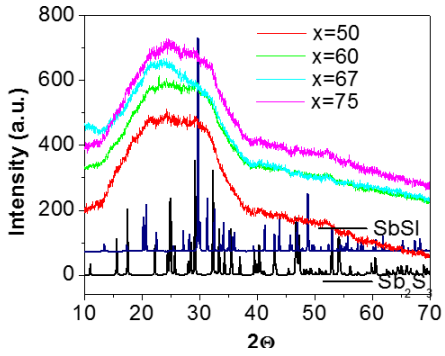


Figure 12. PXRD results of the consolidated product obtained from iodine laden chalcogel with varying weight percentages of $Sb_2S_3$.

*3.10.3.2 Iodine laden chalcogel (SbS-III) consolidation with $As_2S_3$*

Similar to the consolidation experiments with $Sb_2S_3$ four experiments were performed with (a) 50:50, (b) 40:60, (c) 33:67 and (d) 25:75 weight percentage of iodine laden chalcogel and $As_2S_3$ respectively.[20] The experiments were done using the same procedure as above, except the temperature of quenching is 500°C.

The PXRD of the consolidated products in all the four cases with $As_2S_3$ shows the formation of an amorphous phase. The SEM and EDS data shows the presence of Sb, As, S and I in the consolidated product. Around 4 – 17 wt % of iodine could be found in the consolidated product by EDS.

The variation of the amount of iodine (wt %) found in the consolidated product can be understood by taking into account the amount of binary sulfide ($Sb_2S_3$ or $As_2S_3$) added. The expected wt % of iodine along with the observed wt % and % of retention are presented in Table 1. The wt % of the iodine are calculated from the EDS values of the iodine loaded samples before and after heat treatment.

Table 1. Iodine weight % obtained from the EDS data.

| Iodine loaded SbS-III (mg) | $Sb_2S_3$ (mg) | Iodine wt % expected | Iodine wt % found | % Iodine retention |
|---|---|---|---|---|
| 100 | 100 | 33.5 | 27.40 | 81.8 |
| 100 | 150 | 26.8 | 23.28 | 86.9 |
| 100 | 200 | 22.3 | 18.96 | 85.0 |

| | | | | |
|---|---|---|---|---|
| 100 | 300 | 16.75 | 15.90 | 94.9 |
| Iodine loaded SbS-III (mg) | $As_2S_3$ (mg) | Iodine wt % expected | Iodine wt % found | % Iodine retention |
| 100 | 100 | 33.5 | 17.60 | 52.5 |
| 100 | 150 | 26.8 | 9.84 | 36.8 |
| 100 | 200 | 22.3 | 7.77 | 34.8 |
| 100 | 300 | 16.75 | 3.72 | 22.2 |

The wt % of the iodine are calculated from the EDS values and hence it's not an accurate estimation of the iodine present, however, it gives a qualitative idea about the iodine retained in the consolidated product. Around 82 - 95 % of the iodine loaded to the chalcogel could be consolidated in to the final product with $Sb_2S_3$. The obtained high retention of iodine is in agree with its iodine uptake compared to $Sb_2S_3$ powder. However, in case of $As_2S_3$ only 22-53 % of the iodine loaded to the chalcogel could be consolidated.

The consolidation of the iodine loaded chalcogel (SbS-III) with $Sb_2S_3$ powder forms an amorphous phase. The band gap of the consolidated products with varying weight percentages of $Sb_2S_3$ powder was found to be in the range 1.66-1.77 eV from the Uv-Vis/Near-IR spectrum. The Raman spectra of the consolidated products shows four distinct peaks at 107, 141, 250 and 317 $cm^{-1}$. The band gap and the peaks in the Raman spectra are in good agreement with that reported in the literature for the SbSI glass phases.[21-22] Similarly the consolidated products with $As_2S_3$ were also characterized with band gap measurement and Raman spectroscopy. The band gap were found to be in the range 1.96-2.05 eV. The Raman spectra of the consolidated products with $As_2S_3$ shows five distinct peaks at 177, 211, 305, 365 and 491 $cm^{-1}$. The observed band gap and the Raman spectra matches with those reported in the literature for arsenic sulfide glass phases.[23-24]

Figure 13 shows the back scattered detector SEM image of the consolidated products obtained with 50 weight percentage of binary sulfide. The consolidated product obtained with $Sb_2S_3$ appears to have a more homogenous surface with very less silica inclusion (in black) compared to the product obtained with $As_2S_3$.

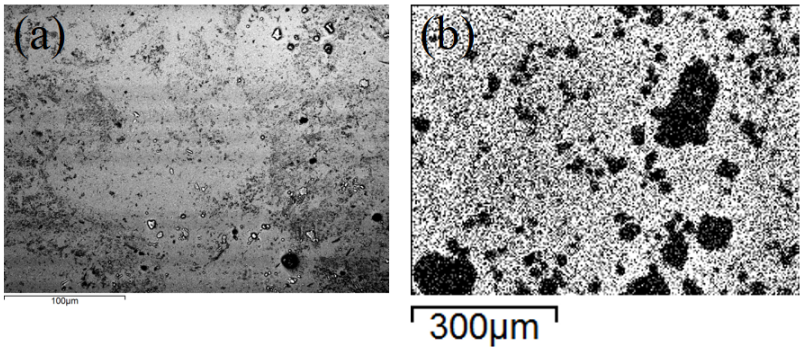


Figure 13. The SEM image of the surface of the consolidated product with (a) 50% $Sb_2S_3$ and (b) 50 % $As_2S_3$.

*3.10.3.3 Targeted glass phase consolidation*

A literature survey gives only one paper where glass formation in the Sb-Sn-S-I system was explored.[25] The glasses were fabricated at 600 °C for 3 hours followed by air quenching. We have targeted four glass composition from the reported Sb-Sn-S-I system by adding required Sn, Sb and $Sb_2S_3$.[17] The target compositions were (a) $Sn_2Sb_{13.6}S_{16.8}I_{7.2}$, (b) $SnSb_{15.3}S_{18.9}I_{8.1}$, (c) $Sn_3Sb_7S_7I_7$ and (d) $Sn_3Sb_9S_9I_9$. In a typical experiments measured amount of iodine laden chalcogel was placed in to a 9 mm diameter fused silica tube and then required Sn, Sb and $Sb_2S_3$ were added on top of the iodine laden materials without mixing. The fused silica ampoules were than evacuated, sealed and heated from room temperature to 650℃ followed by water quenching.

The PXRD of the consolidated product in all the four cases shows the formation of an amorphous phase. The SEM and EDS data shows the presence of Sn, Sb, S and iodine in the consolidated product. Around 20 – 35 wt % of iodine could be found in the consolidated products by EDS (Figure 14).

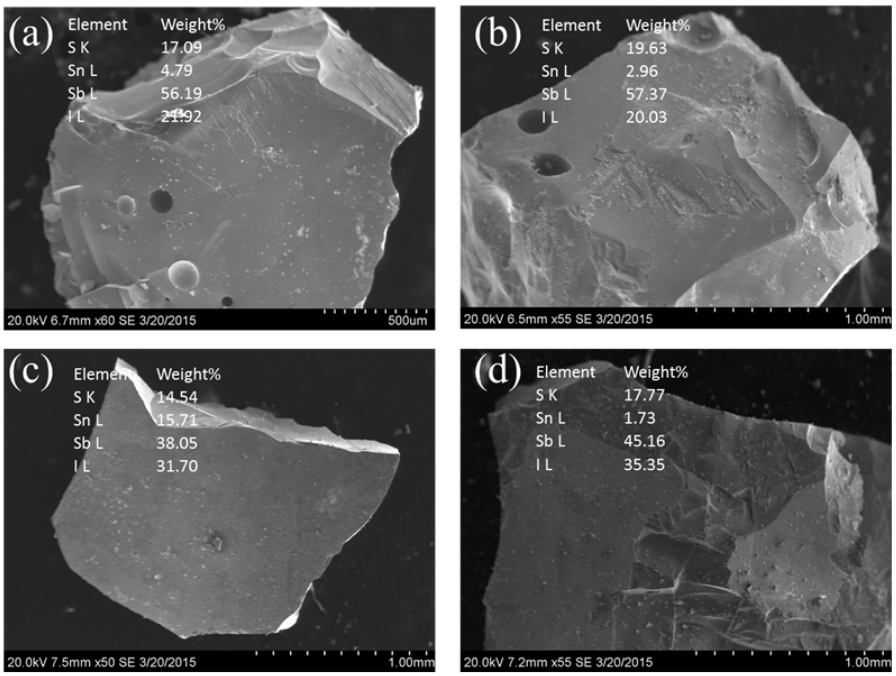


Figure 14. SEM micrograph and EDS data of the consolidated product for the targeted compositions (a) $Sn_2Sb_{13.6}S_{16.8}I_{7.2}$, (b) $SnSb_{15.3}S_{18.9}I_{8.1}$, (c) $Sn_3Sb_7S_7I_7$ and (d) $Sn_3Sb_9S_9I_9$.

The variation of the amount of iodine (wt %) found in the consolidated product can be understood by taking into account the added Sn, Sb and $Sb_2S_3$. The expected wt % of iodine along with the observed wt %, targeted composition and final composition of the experiments are presented in Table 2.

Table 2. Iodine weight % obtained from the EDS data.

| Label | Target | Found | Iodine wt % expected | Iodine wt % found | Iodine wt % retained |
|---|---|---|---|---|---|
| (a) | $Sn_2Sb_{13.6}S_{16.8}I_{7.2}$ | $Sn_2Sb_{12.9}S_{26.4}I_{8.6}$ | 26.3 | 21.92 | 83.3 |
| (b) | $SnSb_{15.3}S_{18.9}I_{8.1}$ | $SnSb_{18.9}S_{24.5}I_{6.3}$ | 23.6 | 20.03 | 84.9 |
| (c) | $Sn_3Sb_7S_7I_7$ | $Sn_3Sb_{7.1}S_{10.2}I_{5.7}$ | 38.2 | 31.7 | 83 |
| (e) | $SnSb_9S_9I_9$ | $SnSb_{25.6}S_{38.2}I_{19.2}$ | 42.7 | 35.35 | 82.8 |

The composition from the EDS showed that two of them are close to the targeted composition. $SnSb_{18.9}S_{24.5}I_{6.3}$ ($SnSb_{15.3}S_{18.9}I_{8.1}$) with a little excess of $Sb_2S_3$ and $Sn_3Sb_{7.1}S_{10.2}I_{5.7}$

($Sn_3Sb_7S_7I_7$) with a little excess of sulfur. The other two composition, $Sn_2Sb_{12.9}S_{26.4}I_{8.6}$ ($Sn_2Sb_{13.6}S_{16.8}I_{7.2}$) and $SnSb_{25.6}S_{38.2}I_{19.2}$ ($SnSb_9S_9I_9$) were found to contain excess sulfur and less tin respectively. However, all the phases was found to be amorphous in nature.

## 4 CONCLUSIONS

A number of novel chalcogels $Zn_2Sn_2S_6$, $Sb_4Sn_4S_{12}$, $NiMoS_4$, $CoMoS_4$, antimony sulfide ($SbS_x$) chalcogels, silver functionalized chalcogels and binary metal sulfides ($Sb_2S_3$) were developed and studies for their iodine absorption efficacies. The iodine in silver functionalized chalcogel is fixed in the form of AgI in the chalcogel matrix, the direct consolidation of the same seems to be a difficult task as the chalcogel matrix tends to decompose. One way to mitigate this is by adding another chalcogenide as a glass forming aid.

The $Sb_2S_3$ powder has a very good iodine uptake capacity (100 wt %) and it absorbs as $SbI_3$. The consolidated product looks promising and the final product is an amorphous phase with 12–21 wt % of iodine. Around 63- 83 % of the absorbed iodine could be consolidated in to the final product.

A number of new antimony sulfide (SbS-I-V) chalcogel were synthesized using simple solution chemistry. These gels absorb light in the near infra-red region exhibiting a band gap of 1.5 eV. Thermal gravimetric analysis indicate that these materials are quite stable. High surface area meso porous aerogels are obtained by drying them super critically. We believe this process is highly saleable. Therefore, these materials with their very promising properties can be further developed for field testing applications in the future. The antimony sulfide chalcogel SbS-III, which is red in color and mesoporous in nature results in a large quantity (200 wt %) of iodine absorption. The consolidated product of the iodine-laden chalcogel with $Sb_2S_3$ is an amorphous phase with 16–27 wt % of iodine and around 82- 95 % of the absorbed iodine could be consolidated in to the final product. Similarly the consolidated product with $As_2S_3$ is also an amorphous phase with 3-17 wt % of iodine and 22- 53 % of the absorbed iodine could be consolidated in to it.

The efforts to optimize the large scale preparation of antimony sulfide chalcogels (SbS-III) were successful. The obtained chalcogel product is fluffy in nature and consists of forests of micro-rods.

The consolidation of the iodine-laden chalcogel (SbS-III) to known glass phases in the Sn-Sb-S-I family is promising. The consolidated products were found to be amorphous in nature with 20–35 wt % of iodine could be consolidated in to the final product.

Robust alginate-chalcogenide composites were also prepared using sodium alginate and SbS/SnS chalcogels and $Sb_2S_3$. This approach leads to the formation of a novel class of chalcogel scaffolds which can be utilized as host matrices to capture iodine in a dynamic mode.

## 5 REFERENCES


1. World Statistics: Nuclear Energy Around the World. http://www.nei.org/Knowledge-Center/Nuclear-Statistics/World-Statistics.

2. Maitra, R. Expand Nuclear Power For the World's Survival. *Executive Intelligence Review* July 25, **2014**, 41-51.

3. Carter, J.; Cozzi, A.; Jones, R.; Matthern , G.; Nutt, M.; Priebe, S.; Sorenson, K. *Global Nuclear Energy Partnership Integrated Waste Management Strategy, GNEP-WAST-WAST-AI-RT-2008-000214, Savannah River National Laboratory, Aiken, SC.* **2008**.

4. Wigeland, R.; Bjornard, T.; Castle, B. *The Concept of Goals-Driven Safeguards, INL/EXT-09-15511, Idaho National Laboratory, Idaho Falls, ID.* **2009**.

5. Murphy, L. P., Staples, B. A., Thomas T. R. The Development of Ag°Z for Bulk $^{129}I$ Removal from Nuclear Fuel Reprocessing Plants and PbX for 129I Storage, ICP-1135, Idaho National Laboratory. **1977**.

6. Bag, S.; Arachchige, I. U.; Kanatzidis, M. G. Aerogels from metal chalcogenides and their emerging unique properties. *J. Mater. Chem.* **2008,** *18*, 3628-3632.

7. Bag, S.; Gaudette, A. F.; Bussell, M. E.; Kanatzidis, M. G. Spongy chalcogels of non-platinum metals act as effective hydrodesulfurization catalysts. *Nat. Chem.* **2009,** *1*, 217-224.

8. Bag, S.; Kanatzidis, M. G. Chalcogels: Porous Metal-Chalcogenide Networks from Main-Group Metal Ions. Effect of Surface Polarizability on Selectivity in Gas Separation. *J. Am. Chem. Soc.* **2010,** *132*, 14951-14959.

9. Bag, S.; Trikalitis, P. N.; Chupas, P. J.; Armatas, G. S.; Kanatzidis, M. G. Porous Semiconducting Gels and Aerogels from Chalcogenide Clusters. *Science* **2007,** *317*, 490-493.

10. Parr, R. G.; Pearson, R. G. Absolute hardness: companion parameter to absolute electronegativity. *J. Am. Chem. Soc.* **1983,** *105*, 7512-7516.

11. Riley, B. J.; Chun, J.; Ryan, J. V.; Matyas, J.; Li, X. S.; Matson, D. W.; Sundaram, S. K.; Strachan, D. M.; Vienna, J. D. Chalcogen-based aerogels as a multifunctional platform for remediation of radioactive iodine. *RSC Adv.* **2011,** *1*, 1704-1715.

12. Riley, B. J.; Chun, J.; Um, W.; Lepry, W. C.; Matyas, J.; Olszta, M. J.; Li, X. H.; Polychronopoulou, K.; Kanatzidis, M. G. Chalcogen-Based Aerogels As Sorbents for Radionuclide Remediation. *Environ. Sci. Technol.* **2013,** *47*, 7540-7547.

13. Riley, B. J.; Pierce, D. A.; Chun, J. *Efforts to consolidate chalcogels with adsorbed iodine. August 2013. PNNL-22678, FCRD-SWF-2013-000249, Pacific Northwest National Laboratory, Richland, WA.* **2013**.

14. Riley, B. J.; Pierce, D. A.; Chun, J.; Matyas, J.; Lepry, W. C.; Garn, T. G.; Law, J. D.; Kanatzidis, M. G. Polyacrylonitrile-Chalcogel Hybrid Sorbents for Radioiodine Capture. *Environ. Sci. Technol.* **2014,** *48*, 5832-5839.

15. Kanatzidis, M. G.; Kota, S. S.; Sarma, D.; Riley, B. J.; Pierce, D. A.; Chun, J. *Novel Metal Sulfides to Achieve Effective Capture and Durable Consolidation of Radionuclides. Jan 2015. Project: 3438, Pacific Northwest National Laboratory, Richland, WA.* **2015**.

16. Kanatzidis, M. G.; Kota, S. S.; Sarma, D.; Riley, B. J.; Pierce, D. A.; Chun, J. *Novel Metal Sulfides to Achieve Effective Capture and Durable Consolidation of Radionuclides. April 2014. Project: 3438, Pacific Northwest National Laboratory, Richland, WA.* **2014**.

17. Kanatzidis, M. G.; Kota, S. S.; Sarma, D.; Riley, B. J.; Pierce, D. A.; Chun, J. *Novel Metal Sulfides to Achieve Effective Capture and Durable Consolidation of Radionuclides. Jul 2015. Project: 3438, Pacific Northwest National Laboratory, Richland, WA.* **2015**.

18. Kanatzidis, M. G.; Kota, S. S.; Sarma, D.; Riley, B. J.; Pierce, D. A.; Chun, J. *Novel Metal Sulfides to Achieve Effective Capture and Durable Consolidation of Radionuclides. Oct 2015. Project: 3438, Pacific Northwest National Laboratory, Richland, WA.* **2015**.

19. Kanatzidis, M. G.; Sarma, D.; Kota, S. S.; Riley, B. J.; Pierce, D. A.; Chun, J. *Novel Metal Sulfides to Achieve Effective Capture and Durable Consolidation of Radionuclides. July 2014. Project: 3438, Pacific Northwest National Laboratory, Richland, WA.* **2014**.

20. Kanatzidis, M. G.; Sarma, D.; Kota, S. S.; Riley, B. J.; Pierce, D. A.; Chun, J. *Novel Metal Sulfides to Achieve Effective Capture and Durable Consolidation of Radionuclides. April 2015. Project: 3438, Pacific Northwest National Laboratory, Richland, WA.* **2015**.

21. Ding, L.; Zhao, D.; Jain, H.; Xu, Y.; Wang, S.; Chen, G. Structure of $GeS_2$–SbSI Glasses by Raman Spectroscopy. *J. Am. Ceram. Soc.* **2010,** *93*, 2932-2934.

22. Turyanitsa, I. D.; Vodop'yanov, L. K.; Rubish, V. M.; Kengerlinskii, L. Y.; Dobosh, M. V. Raman spectra and dielectric properties of glasses of the Sb-S-I system. *J. Appl. Spectrosc.* **1986,** *44*, 501-504.

23. Frumar, M.; Jedelský, J.; Frumarová, B.; Wágner, T.; Hrdlička, M. Optically and thermally induced changes of structure, linear and non-linear optical properties of chalcogenides thin films. *J. Non-Cryst. Solids* **2003,** *326–327*, 399-404.

24. Lyubin, V. M.; Tikhomirov, V. K. Novel photo-induced effects in chalcogenide glasses. *J. Non-Cryst. Solids* **1991,** *135*, 37-48.

25. Turyanitsa, I. D.; Migolinets, I. M.; Koperles, B. M.; Kopinets, I. F. Glasses in tin-antimony-sulfur-iodine and lead-antimony-sulfur-iodine systems. *Izv. Akad. Nauk SSSR, Neorg. Mater.* **1974,** *10*, 1436-1438.

## 6 PUBLICATIONS

The following articles were published from the support of this NEUP grant from the Department of Energy, Office of Nuclear Energy.

1. Mertz, J. L.; Fard, Z. H.; Malliakas, C. D.; Manos, M. J.; Kanatzidis, M. G. Selective Removal of $Cs^{+}$, $Sr^{2+}$, and $Ni^{2+}$ by $K_{2x}Mg_xSn_{3-x}S_6$ (x = 0.5–1) (KMS-2) Relevant to Nuclear Waste Remediation. *Chem. Mater.* **2013**, *25*, 2116-2127.

2. Riley, B. J.; Chun, J.; Um, W.; Lepry, W. C.; Matyas, J.; Olszta, M. J.; Li, X.; Polychronopoulou, K.; Kanatzidis, M. G. Chalcogen-Based Aerogels As Sorbents for Radionuclide Remediation. *Environ. Sci. Technol.* **2013**, *47*, 7540-7547.

3. Ma, S.; Islam, S. M.; Shim, Y.; Gu, Q.; Wang, P.; Li, H.; Sun, G.; Yang, X.; Kanatzidis, M. G. Highly Efficient Iodine Capture by Layered Double Hydroxides Intercalated with Polysulfides. *Chem. Mater.* **2014**, *26*, 7114-7123.

4. Islam, S. M.; Subrahmanyam, K. S.; Malliakas, C. D.; Kanatzidis, M. G. One-Dimensional Molybdenum Thiochlorides and Their Use in High Surface Area MoSx Chalcogels. *Chem. Mater.* **2014**, *26*, 5151-5160.

5. Riley, B. J.; Pierce, D. A.; Chun, J.; Matyáš, J.; Lepry, W. C.; Garn, T. G.; Law, J. D.; Kanatzidis, M. G. Polyacrylonitrile-Chalcogel Hybrid Sorbents for Radioiodine Capture. *Environ. Sci. Technol.* **2014**, *48*, 5832-5839.

6. Ma, S.; Huang, L.; Ma, L.; Shim, Y.; Islam, S. M.; Wang, P.; Zhao, L.-D.; Wang, S.; Sun, G.; Yang, X.; Kanatzidis, M. G. Efficient Uranium Capture by Polysulfide/Layered Double Hydroxide Composites. *J. Am. Chem. Soc.* **2015**, *137*, 3670-3677.

8. Riley, B. J.; Pierce, D. A.; Lepry, W. C.; Kroll, J. O.; Chun, J.; Subrahmanyam, K. S.; Kanatzidis, M. G.; Alblouwy, F. K.; Bulbule, A.; Sabolsky, E. M. Consolidation of Tin Sulfide Chalcogels and Xerogels with and without Adsorbed Iodine. *Ind. Eng. Chem. Res.* **2015**, *54*, 11259-11267.

9. Subrahmanyam, K. S.; Sarma, D.; Malliakas, C. D.; Polychronopoulou, K.; Riley, B. J.; Pierce, D. A.; Chun, J.; Kanatzidis, M. G. Chalcogenide Aerogels as Sorbents for Radioactive Iodine. *Chem. Mater.* **2015**, *27*, 2619-2626.

10. Subrahmanyam, K. S.; Malliakas, C. D.; Sarma, D.; Armatas, G. S.; Wu, J.; Kanatzidis, M. G. Ion-Exchangeable Molybdenum Sulfide Porous Chalcogel: Gas Adsorption and Capture of Iodine and Mercury. *J. Am. Chem. Soc.* **2015**, *137*, 13943-13948.

11. Sarma, D.; Malliakas, C. D.; Subrahmanyam, K. S.; Islam, S. M.; Kanatzidis, M. G. $K_{2x}Sn_{4-x}S_{8-x}$ (x = 0.65-1): a new metal sulfide for rapid and selective removal of $Cs^{+}$, $Sr^{2+}$ and $UO_2^{2+}$ ions. *Chem. Sci.* **2016**, *7*, 1121-1132.